

# Nuclear Fermi Momenta of $^2\text{H}$ , $^{27}\text{Al}$ and $^{56}\text{Fe}$ from an Analysis of CLAS data

Hui Liu,<sup>1,2,\*</sup> Na-Na Ma,<sup>3,†</sup> and Rong Wang<sup>1,4,‡</sup>

<sup>1</sup>*Institute of Modern Physics, Chinese Academy of Sciences, Lanzhou 730000, China*

<sup>2</sup>*School of Fundamental Physics and Mathematical Sciences,*

*Hangzhou Institute for Advanced Study, UCAS, Hangzhou 310024, China*

<sup>3</sup>*School of Nuclear Science and Technology, Lanzhou University, Lanzhou 730000, China*

<sup>4</sup>*University of Chinese Academy of Sciences, Beijing 100049, China*

(Dated: March 1, 2025)

Nuclear Fermi momentum is a basic property of a nucleus where many nucleons dwell. However, in experiments only the nuclear Fermi momenta of just a few nuclei are measured using the electron quasielastic scattering off the nucleus so far. Particularly, we still do not know experimentally the Fermi momentum of the lightest nucleon composite – the deuteron. In this paper, we apply a gaussian distribution to describe the quasielastic peak in the cross section of electron-nucleus scattering. By performing the least-square fits to the recent CLAS data in the narrow quasielastic region, we obtain the nuclear Fermi momenta of  $^2\text{H}$ ,  $^{27}\text{Al}$  and  $^{56}\text{Fe}$ , which are  $116 \pm 4$  MeV/c,  $237 \pm 13$  MeV/c, and  $241 \pm 13$  MeV/c respectively. The extracted nuclear Fermi momenta are compared to the simple calculations using Fermi gas model, and the consistences are found.

## I. INTRODUCTION

An atomic nucleus is a compact system composed of nucleon fermions – protons and neutrons – under the strong nuclear force. The Fermi statistic can be used to describe the single particle motion inside the nucleus. The nuclear Fermi momentum is used to describe the independent nucleon energy level near Fermi surface. In a nucleus, the nucleons move with an average momentum which is closely related to the nuclear Fermi momentum. The motions of the nucleons affect the scattering processes under the high momentum transfer, such as the quasielastic scattering [1–5], the transverse momentum spectrum [6–8] and the deep inelastic scattering [9–12]. What’s more? The better understanding of the nuclear Fermi momentum helps us better searching the high momentum tail of the nucleon momentum distribution and the short-range correlations among the nucleons [13–17], since the quasielastic scattering is sensitive to both the single nucleon motion and the nucleon-nucleon correlations.

The nuclear Fermi momentum can be deduced via the quasielastic scattering of a high energy electron off the nuclear target [1–3], due to the weakly electromagnetic interaction which does not disturb much the structure of the target. The quasielastic scattering can simply be viewed as the electron scatters from an individual and moving nucleon in the Fermi sea, with the recoiling nucleon going outside of the Fermi sphere (escaping from the nucleus for the most cases). A quasielastic peak dominates in the spectrum of the electron energy loss below the continuum region caused by deep inelastic scattering. The width of the quasielastic peak is broadened by the

Fermi motion of the nucleons, and the position of the peak is affected by the separation energy between the struck nucleon and remanent nucleus [1–3]. Therefore measuring the width of the quasielastic peak is the key of extracting the nuclear Fermi momentum. Usually the differential cross section of quasielastic scattering is described with the spectral function  $S(\vec{k}, E)$ , where  $\vec{k}$  and  $E$  are the initial momentum and the initial energy of the struck nucleon respectively [5]. In the plane wave impulse approximation, the famous  $y$ -scaling for quasielastic scattering implies the nucleonic degrees of freedom and the initial nucleon momentum distribution [5, 18–21].

Nuclear Fermi momentum is important for us to study the properties of the nucleon in the experiments using the nuclear targets. Recent high precision data of electron-nucleus quasielastic scattering is provided by the CLAS collaboration with the facilities at JLab [22]. Hence it is interesting to look at the quasielastic scattering peak at  $x_B = \frac{Q^2}{2m\omega} \sim 1$ , where  $Q^2$  and  $\omega$  are the minus four-momentum square and the energy of the exchanged virtual photon respectively. We use a simple Fermi smearing model in explaining the experimental data and try to extract the nuclear Fermi momentum of some unmeasured nuclei. The method is discussed in Sec. II. The determination of the deuteron Fermi momentum is shown in Sec. III. The determinations of the nuclear Fermi momenta of aluminium and iron are shown in Sec. IV. Some discussions and a concise summary is given in Sec. V.

## II. A GAUSSIAN MODEL FOR THE QUASIELASTIC SCATTERING PEAK

The quasielastic scattering off a nucleus is viewed as the elastic scattering between the electron probe and one nucleon inside the nucleus. Compared to the e-p elastic scattering, the energy transfer at certain angle in the quasielastic scattering is smeared by the nucleon Fermi motion. To depict the smearing from the randomly mov-

\* liuhui@impcas.ac.cn

† mann15@lzu.edu.cn

‡ rwang@impcas.ac.cn (corresponding author)

ing nucleon, we apply a naive gaussian distribution for the simplicity. It turns out to be fine in the narrow range of the quasielastic peak.

The differential cross section of the nuclear quasielastic scattering over the energy transfer  $\omega$  is modeled as,

$$\frac{1}{A} \frac{d\sigma_A(\omega)}{d\omega} = \sigma_{eN} \frac{1}{\sqrt{2\pi}ck_{F,A}} e^{-\frac{(\omega-\omega_0)^2}{2c^2k_{F,A}^2}}, \quad (1)$$

where  $A$  is the mass number of the nucleus,  $\omega = E - E'$  is the energy transfer from the electron to the nucleon, and  $\sigma_{eN}$  represents the total cross section of e-N elastic scattering. The main assumption of our model is that the width for the differential cross section smearing is proportional to the nucleon Fermi momentum  $k_{F,A}$  inside the nucleus  $A$  [1–3]. Therefore, in Eq. (1), we introduce a pure coefficient  $c$ , which a universal constant for all the nuclear targets in the same experiment.

In experiment, we usually present the cross-section as a function of the Bjorken scaling variable  $x_B$ . In the nuclear target rest frame, the energy exchange  $\omega$  is connected to  $x_B$ , via the definition of the Bjorken scaling variable.  $\omega$  is related to  $x_B$  as,

$$\omega = \frac{Q^2}{2mx_B}, \quad (2)$$

where  $Q^2$  is the square of four-momentum transfer and  $m$  is the nucleon mass. Note that  $x_B = 1$  corresponds to the peak of the differential cross-section of quasielastic scattering with a slightly shift, and this shift of the peak comes from the average nucleon separation energy [1–3]. Again the gaussian smearing model doesn't work far from  $x_B = 1$ . Using Eq. (2), we can rewrite the per-nucleon quasielastic cross section as a function of  $x_B$ , which is written as,

$$\begin{aligned} \frac{1}{A} \frac{d\sigma_A(x_B)}{dx_B} &= \left| \frac{1}{A} \frac{d\sigma_A(\omega)}{d\omega} \frac{d\omega}{dx_B} \right| \\ &= \frac{\sigma_{eN}}{\sqrt{2\pi}ck_{F,A}} \exp \left[ -\frac{(\frac{1}{x_B} - X_0)^2}{2W_A^2} \right] \frac{Q^2}{2mx_B^2}, \end{aligned} \quad (3)$$

where we have  $X_0 = \frac{2m\omega_0}{Q^2}$  for the central value and  $W_A = \frac{2mck_{F,A}}{Q^2}$  for the width. With  $A = 2$  in Eq. (3), we get the quasielastic cross-section for deuteron. Divide the quasielastic scattering of a heavy nucleus by that of deuteron, we then get a master formula for the cross-section ratio near  $x_B \sim 1$ ,

$$\left| \frac{d\sigma_A/A}{d\sigma_D/2} \right| = \frac{W_D}{W_A} \exp \left[ \frac{(\frac{1}{x_B} - X_0)^2}{2W_D^2} - \frac{(\frac{1}{x_B} - X_0)^2}{2W_A^2} \right] \quad (4)$$

Here the subscript D means deuteron. Note that  $W_A = \frac{2mck_{F,A}}{Q^2}$  is linearly proportional to the nuclear Fermi momentum of the nucleus  $A$ . Once the  $W_{A_1}/W_{A_2}$  is extracted from the data of the cross-section ratio, the Fermi momentum ratio of two nuclei is also obtained. In Eq.

(4), the free parameter  $X_0$  should be 1 for elastic scattering. Due to the mass deficit of the nucleon inside the nucleus, the calculation of  $x_B$  is different for the bound nucleon, hence the parameter  $X_0$  is slightly away from 1. In this analysis, we let  $X_0$  be a free and universal parameter for all the nuclei, since the masses of the bound nucleon in different nuclei are almost the same, and the value of  $X_0$  would not affect the width of the quasielastic peak.

The Fermi momenta of several nuclei were measured decades ago [2], such as  $^{12}\text{C}$  and  $^{208}\text{Pb}$ . Recently the quasielastic cross-section ratio of some heavy nuclei ( $^{12}\text{C}$ ,  $^{27}\text{Al}$ ,  $^{56}\text{Fe}$ , and  $^{208}\text{Pb}$ ) to deuteron are analyzed by CLAS Collaboration in the data-mining project of 6 GeV data [22]. Therefore this provide an opportunity to determine the Fermi momentum of deuteron, combing the measurements above, with the model expressed in Eq. (4). The main purpose of the paper is to provide the Fermi momenta of some unmeasured nuclei based on the Fermi motion smearing model.

### III. FERMI MOMENTUM OF DEUTERON

Fig. 1 and Fig. 2 show the per-nucleon quasielastic cross-section ratios as a function of  $x_B$  [22], for  $^{12}\text{C}$  nucleus over deuteron and for  $^{208}\text{Pb}$  nucleus over deuteron, respectively. The least-square fits based on the model described in Eq. (4) are performed to the data and shown in the figures. The qualities of the fits indicate a good consistency between the model and the experimental data. In the fits, we let  $X_0$ ,  $W_A$  and  $W_D/W_A$  be the free parameters.  $W_D/W_C$  is determined to be  $0.5174 \pm 0.0096$ , and  $W_D/W_{Pb}$  is determined to be  $0.4421 \pm 0.0083$ .

The ratio of the quasielastic peak width actually can be viewed as the ratio of the nuclear Fermi momentum. As the nuclear Fermi momenta of carbon and lead are already determined to be  $221 \pm 5$  MeV/c and  $265 \pm 5$  MeV/c respectively from the previous measurements [2], we then deduce the nuclear Fermi momentum of deuteron to be  $114 \pm 5$  MeV/c and  $117 \pm 5$  MeV/c from the obtained ratios of quasielastic peak widths. It is delighting to find that the Fermi momenta of deuteron obtained from the cross-section ratios of different nuclear targets are consistent with each other within the uncertainty. To get an average, the Fermi momentum of deuteron is combined to be  $116 \pm 4$  MeV/c.

### IV. FERMI MOMENTA OF ALUMINIUM AND IRON

The quasielastic scattering cross-section ratio between other heavy nuclei and deuteron are also measured by CLAS Collaboration. Fig. 3 shows the cross-section ratio between  $^{27}\text{Al}$  and  $^2\text{H}$ ; And Fig. 4 shows the cross-section ratio between  $^{56}\text{Fe}$  and  $^2\text{H}$ . By performing the fits to the CLAS data, we have obtained the quasielastic peak width

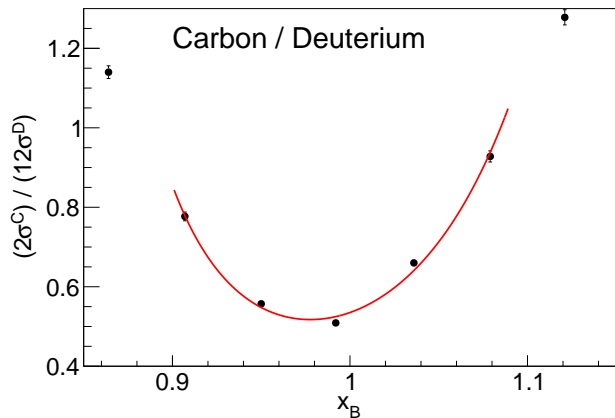


FIG. 1. The quasielastic cross-section ratio  $\left| \frac{d\sigma_{\Lambda/A}}{d\sigma_{\text{D}/2} \right|$  of carbon to deuteron as a function of the Bjorken variable  $x_B$ . The experimental data are taken from CLAS Collaboration [22]. The curve shows a fit to a model of the assumption that the quasielastic peak is gaussian. The fit quality is  $\chi^2/N = 11/5$ .

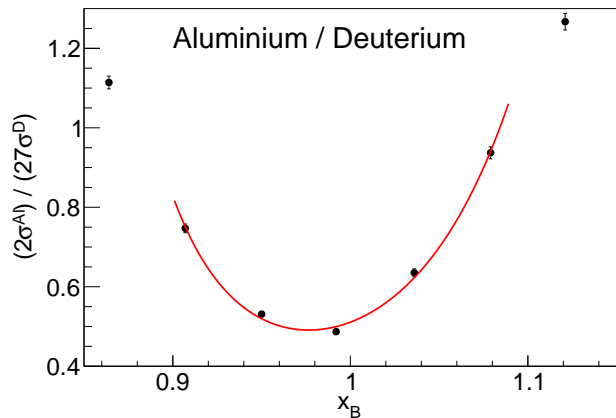


FIG. 3. The quasielastic cross-section ratio  $\left| \frac{d\sigma_{\Lambda/A}}{d\sigma_{\text{D}/2} \right|$  of aluminium to deuteron as a function of the Bjorken variable  $x_B$ . The experimental data are taken from CLAS Collaboration [22]. The curve shows a fit to a model of the assumption that the quasielastic peak is gaussian. The fit quality is  $\chi^2/N = 7.0/5$ .

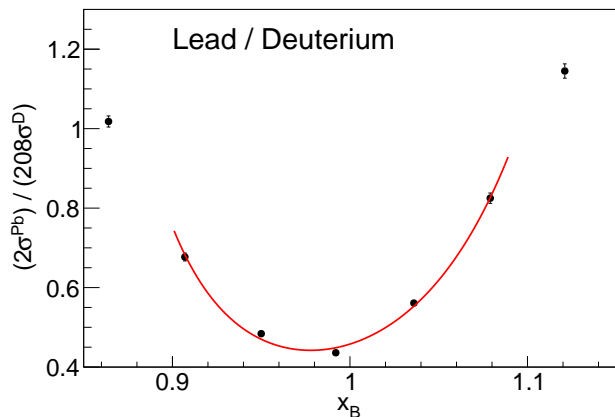


FIG. 2. The quasielastic cross-section ratio  $\left| \frac{d\sigma_{\Lambda/A}}{d\sigma_{\text{D}/2} \right|$  of lead to deuteron as a function of the Bjorken variable  $x_B$ . The experimental data are taken from CLAS Collaboration [22]. The curve shows a fit to a model of the assumption that the quasielastic peak is gaussian. The fit quality is  $\chi^2/N = 9.6/5$ .

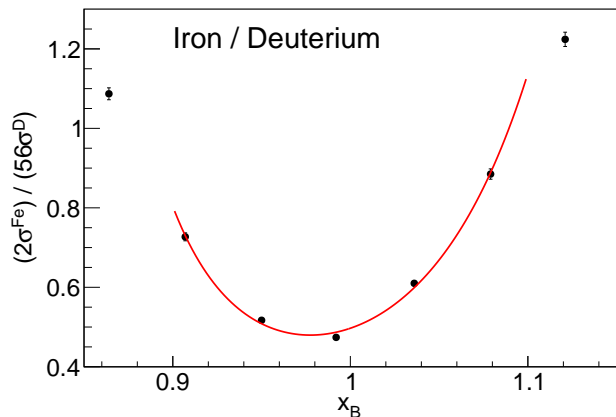


FIG. 4. The quasielastic cross-section ratio  $\left| \frac{d\sigma_{\Lambda/A}}{d\sigma_{\text{D}/2} \right|$  of iron to deuteron as a function of the Bjorken variable  $x_B$ . The experimental data are taken from CLAS Collaboration [22]. The curve shows a fit to a model of the assumption that the quasielastic peak is gaussian. The fit quality is  $\chi^2/N = 6.6/5$ .

ratios:  $W_{\text{Al}}/W_{\text{D}} = 2.04 \pm 0.04$  and  $W_{\text{Fe}}/W_{\text{D}} = 2.08 \pm 0.04$ .

The width ratio directly equals to the nuclear Fermi momentum ratio. Since we have determined the Fermi momentum of deuteron in the above section, we can calculate the Fermi momentum of other heavy nuclei from the obtained Fermi momentum ratios. Based on the outcome of the above analysis, we have determined the Fermi momenta of  $^{27}\text{Al}$  and  $^{56}\text{Fe}$ , which are summarized in Table I.

## V. DISCUSSIONS AND SUMMARY

From our analysis based on a simple model, we find that the nuclear Fermi momentum of deuteron is less than half of that of heavy nucleus, while the Fermi momenta of aluminium and iron are close to the Fermi momentum of heavy nuclei around 250 MeV/c. An interesting question is that whether or not the Fermi motion of the nucleon in deuteron satisfies the Fermi gas model description.

In Fermi gas model, the Fermi momentum is directly

TABLE I. Fermi Momenta of some nuclei determined in this work.  $k_{F, \text{exp.}}$  denotes the Fermi momentum given by our analysis of the CLAS data. The errors are the statistical errors only.  $k_{F, \text{theo.}}$  denotes the Fermi momentum given by the calculation from the Fermi gas model for the nucleus (see Eq. (7)).

Nucleus	$k_{F, \text{exp.}}$ (MeV/c)	$k_{F, \text{theo.}}$ (MeV/c)
$^2\text{H}$	$116 \pm 4$	140
$^{27}\text{Al}$	$236 \pm 13$	226
$^{56}\text{Fe}$	$241 \pm 13$	231

connected to the nuclear density. Based on the Pauli exclusion principle, the nucleon fermions fully occupy the quantum states in the nucleus. Assuming a sphere nucleus, the number of nucleon fermions is simply counted as [23],

$$\tilde{n} = 2 \frac{\left(\frac{4}{3}\pi R^3\right) \left(\frac{4}{3}\pi k_F^3\right)}{(2\pi\hbar)^3}, \quad (5)$$

where  $\tilde{n}$  is the proton number or the neutron number,  $R$  is the radius of a nucleus and  $k_F$  is the Fermi momentum. Approximately the nuclear radius is proportional to  $A^{1/3}$ . With  $R = r_0 A^{1/3}$ , the proton Fermi momentum  $k_F^p$  in Fermi gas model is calculated as,

$$k_F^p = \frac{1}{r_0} \left( \frac{9}{4} \pi \frac{Z}{A} \right)^{\frac{1}{3}}, \quad (6)$$

in which  $\hbar$  equals to one with the natural unit used. Using the formula  $\rho = A/(\frac{4}{3}\pi R^3)$ , we can rewrite the proton Fermi momentum as a function of the nuclear density  $\rho$ , which is written as,

$$k_F^p = \left( 3\pi^2 \frac{Z}{A} \rho \right)^{\frac{1}{3}}. \quad (7)$$

Here we assume a spherical nucleus and we set  $\hbar$  to 1 with the natural unit used.

We adopt the nuclear density data from Ref. [24] (see Table II for the nuclei studied in this paper). These average nuclear densities are calculated with  $\rho(A) = 3A/(4\pi R_e^3)$  and  $R_e^2 = 5 \langle r^2 \rangle / 3$ .  $\langle r^2 \rangle$  is the root-mean-square radius from the electron elastic scattering off the nucleus [24].

TABLE II. Nucleon densities of some nuclei [24].

A	$^2\text{H}$	$^{12}\text{C}$	$^{27}\text{Al}$	$^{56}\text{Fe}$
$\rho$ (fm $^{-3}$ )	0.024	0.089	0.106	0.117

With the density of  $^{12}\text{C}$ , the Fermi momentum of  $^{12}\text{C}$  is 216 MeV/c based on the Fermi gas model described above, which is consistent with the experimental measured value  $221 \pm 25$  MeV/c [2]. The Fermi gas model predictions for other nuclei are listed in Table I. We found that the Fermi momenta of  $^{27}\text{Al}$  and  $^{56}\text{Fe}$  extracted in this work agree well with the Fermi gas model calculations, while the Fermi momentum of deuteron is slightly smaller than the model prediction. This implies that the Fermi gas model may not work for the very light nucleus. Moreover, the determined Fermi momentum of deuteron is larger than the prediction 87 MeV/c from a phenomenological parametrization [25], with  $k_F(Z, N, A) = k_F^p(1 - A^{-t_p})\frac{Z}{A} + k_F^n(1 - A^{-t_n})\frac{N}{A}$ .

The Fermi momentum of deuteron is extracted for the first time from the quasielastic scattering data from CLAS [22]. The Fermi momentum of deuteron is  $116 \pm 4$  MeV/c, which much smaller than that of the nuclei of high density. The good fits of our model to the data indicate that the gaussian distribution is valid to fit the quasielastic cross-section in a narrow range, and the width of the quasielastic peak is proportional to the nuclear Fermi momentum. The cross-section ratio for quasielastic scattering can be described with the formula in Eq. (4). Within this formulism and the CLAS data, we have extracted the Fermi momenta of two unmeasured heavy nuclei,  $^{27}\text{Al}$  and  $^{56}\text{Fe}$ .

The quasielastic scattering by the high energy electron beam off the nuclei is not only an important tool to see the short-range correlations among nucleons, but also a powerful method to acquire the information of nucleon Fermi motion inside the nuclei. And these nucleon Fermi motion information would be very helpful to the analysis of the experiments with the nuclear targets to study the neutrons or the protons (such as the deuteron target). Last but not least, to understand the Fermi momenta of light nuclei we need more theoretical and experimental studies.

## ACKNOWLEDGMENTS

This work is supported by the National Natural Science Foundation of China under the Grant NO. 12005266 and the Strategic Priority Research Program of Chinese Academy of Sciences under the Grant NO. XDB34030301.

[1] E. J. Moniz, Phys. Rev. **184**, 1154 (1969).

[2] E. J. Moniz, I. Sick, R. R. Whitney, J. R. Ficenece, R. D.

- Kephart, and W. P. Trower, Phys. Rev. Lett. **26**, 445 (1971).
- [3] R. R. Whitney, I. Sick, J. R. Ficenec, R. D. Kephart, and W. P. Trower, Phys. Rev. C **9**, 2230 (1974).
- [4] T. W. Donnelly and J. D. Walecka, Ann. Rev. Nucl. Part. Sci. **25**, 329 (1975).
- [5] O. Benhar, D. day, and I. Sick, Rev. Mod. Phys. **80**, 189 (2008), arXiv:nucl-ex/0603029.
- [6] S. Fredriksson, Nucl. Phys. B **94**, 337 (1975).
- [7] S. Fredriksson, Nucl. Phys. B **111**, 167 (1976).
- [8] G.-C. Yong, Phys. Lett. B **765**, 104 (2017), arXiv:1503.08523 [nucl-th].
- [9] K. Saito and T. Uchiyama, Z. Phys. A **322**, 299 (1985).
- [10] M. Arneodo, Phys. Rept. **240**, 301 (1994).
- [11] D. F. Geesaman, K. Saito, and A. W. Thomas, Ann. Rev. Nucl. Part. Sci. **45**, 337 (1995).
- [12] S. Malace, D. Gaskell, D. W. Higinbotham, and I. Cloet, Int. J. Mod. Phys. E **23**, 1430013 (2014), arXiv:1405.1270 [nucl-ex].
- [13] J. Arrington, D. W. Higinbotham, G. Rosner, and M. Sargsian, Prog. Part. Nucl. Phys. **67**, 898 (2012), arXiv:1104.1196 [nucl-ex].
- [14] O. Hen, G. A. Miller, E. Piasetzky, and L. B. Weinstein, Rev. Mod. Phys. **89**, 045002 (2017), arXiv:1611.09748 [nucl-ex].
- [15] O. Hen et al., Science **346**, 614 (2014), arXiv:1412.0138 [nucl-ex].
- [16] A. Schmidt et al. (CLAS), Nature **578**, 540 (2020), arXiv:2004.11221 [nucl-ex].
- [17] X. G. Wang, A. W. Thomas, and W. Melnitchouk, Phys. Rev. Lett. **125**, 262002 (2020), arXiv:2004.03789 [hep-ph].
- [18] G. B. West, Phys. Rept. **18**, 263 (1975).
- [19] I. Sick, D. Day, and J. S. McCarthy, Phys. Rev. Lett. **45**, 871 (1980).
- [20] D. B. Day et al., Phys. Rev. Lett. **59**, 427 (1987).
- [21] J. Arrington et al., Phys. Rev. C **53**, 2248 (1996), arXiv:nucl-ex/9504003.
- [22] B. Schmookler et al. (CLAS), Nature **566**, 354 (2019).
- [23] S. D'Auria, Introduction to Nuclear and Particle Physics (Springer, 2019).
- [24] J. Gomez et al., Phys. Rev. D **49**, 4348 (1994).
- [25] R. Wang, X. Chen, and Q. Fu, Nucl. Phys. B **920**, 1 (2017), arXiv:1611.03670 [hep-ph].